Journal of Water Process Engineering 4 (2014) 12–24

Contents lists available at ScienceDirect

Journal of Water Process Engineering

journal homepage: www.elsevier.com/locate/jwpe

Chemically activated carbon residue from biomass gasification as a sorbent for iron(II), copper(II) and nickel(II) ions

Hanna Runtti [a], Sari Tuomikoski [a], Teija Kangas [a], Ulla Lassi [a,b,*], Toivo Kuokkanen [a], Jaakko Rämö [c]

[a] University of Oulu, Department of Chemistry, P.O. Box 3000, FI-90014, Finland
[b] University of Oulu, Kokkola University Consortium Chydenius, Unit of Applied Chemistry, P.O. Box 567, FI-67100 Kokkola, Finland
[c] Thule Institute, University of Oulu, P.O. Box 7300, FI-90014, Finland

ARTICLE INFO

Article history:
Received 22 March 2014
Received in revised form 26 August 2014
Accepted 27 August 2014

Keywords:
Sorption
Heavy metals
Chemical activation
Carbon residue
Activated carbon

ABSTRACT

The main goal of this research was to investigate the possibility of the utilization of carbon residue from biomass gasification process with and without chemical activation as a low cost sorbent for iron(II), copper(II) and nickel(II) ions from an aqueous solution. Commercial activated carbon was used as a reference sample. Batch experiments were done to evaluate the influence of pH, initial metal concentration and contact time. The optimum pH required for maximum adsorption was found to be 4, 5 and 8, for iron, copper and nickel, respectively. According to the results, the removal of metals by carbon residue with and without chemical activation was higher than commercial activated carbon. The highest maximum experimental sorption capacities ($q_{m,exp}$) for iron, copper and nickel by activated carbon residue were 21, 23 and 18 mg g^{-1}, respectively. The experimental equilibrium sorption data were tested for the Langmuir, Freundlich and Dubinin–Radushkevich (D–R) equations. Depending on the system the Langmuir or Freundlich isotherms have been found to provide the best correlation. The kinetics of iron, copper and nickel sorption by different adsorbent materials followed the pseudo-second-order model. Other tested kinetic models were the pseudo-first-order and the Elovich models. Weber Morris's intraparticle diffusion model showed that there are two or three different stages for the removal of metals.

1. Introduction

Heavy metals are examples of toxic pollutants that are known to be released into the environment from many industries such as mining, tanneries, painting, metal plating, battery industry and from agricultural sources. These metals tend to accumulate in ecological systems causing serious soil and water pollution which can also be harmful to human, animals and plants even in low concentrations. At high doses, iron can cause rapid pulse rates, congestion of blood vessels and hypertension. Copper can cause for example nausea, diarrhea, respiratory difficulties, liver and kidney failure. Nickel is also a toxic metal and at high concentrations can lead for example to skin dermatitis, nausea and cancer of lungs, nose and bone [1,2]. In Table 1 different permissible limits for potable waters and industrial effluents for iron, copper and nickel are showed [3–6].

Numerous techniques have been reported for the removal of heavy metals from industrial effluents and wastewaters that often involve a combination of different processes to achieve the desired water quality. For instance, technologies such as ion exchange [7], chemical precipitation [8], membranes (e.g. ultrafiltration, reverse osmosis and electrodialysis) [9–11], liquid extraction [12] and flotation [13] are useful for heavy metal removal. These methods are often ineffective or involve expensive techniques. A case in point, membrane techniques can effectively reduce metal ions to a very low level but are less commonly used due to their high operational cost. In addition, precipitation is considered the most economical method but this technique produces a large amount of precipitate sludge that requires further treatment [1].

Adsorption is possible and commonly used method for the removal of heavy metals from an aqueous solution due to its high efficiency, cost-efficient technique and simple operation. Adsorption processes using commercial activated carbon are widely used to remove pollutants from wastewaters. However, the high cost of activated carbon inhibits sometimes its widespread use in wastewater treatments and therefore there is a need to develop other adsorbents from alternative low-cost raw materials. Over the last

* Corresponding author at: University of Oulu, Department of Chemistry, P.O. Box 3000, FI-90014, Finland. Tel.: +358 40 029 4090.
E-mail address: ulla.lassi@oulu.fi (U. Lassi).

http://dx.doi.org/10.1016/j.jwpe.2014.08.009
2214-7144/

Table 1
Permissible limits of iron, copper and nickel ions for potable waters and industrial effluents [3–6].

Metal	Potable water (mg L^{-1})			Industrial effluent discharge (mg L^{-1})	
	EU standard	USEPA	WHO	HELCOM (20E/6, 1999)	WHO Inland surface water
Fe	0.2	0.3	0.3	–	0.1–1.0
Cu	2.0	1.3	2.0	≤0.5	0.05–1.5
Ni	0.02	0.1	0.02	≤1.0	–

few years, a number of low-cost adsorbents produced from waste biomass (e.g. olive stone waste, saw dust, peanut hulls) [14–17], industrial waste (e.g. fly ash, waste sludge, red mud) [18–20] and mineral waste (e.g. coal, kaolinite, bentonite) [21–23] have been reported for the removal of metallic pollutants from water and wastewater [1,24].

Climate change is one of the most serious environmental problems in the world today. Therefore energy generation from biomass has become more common and popular in recent years [25]. Biomass gasification is used for generating energy (heat and power) from different types of organic materials and it is one of the most effective energy conversion technologies for the utilization of biomass [26]. Syngas produced from biomass gasification can be used directly as fuel for an internal combustion engine or as a chemical feedstock to produce liquid fuels by the Fischer–Tropsch method [27]. It can be assumed that the biomass gasification will only increase in the future and therefore the amount of solid residues formed in the gasification process will also increase [25]. According to the European strategy on waste materials [28], all kinds of waste must be utilized primarily as material (reuse and recycling), secondary as energy and if neither of those utilization methods are possible, they can be disposed via ecologically beneficial methods. The different options available for dealing with waste can be described by a waste hierarchy which is derived from five categories; i.e. prevention, reuse and preparation for reuse, recycling, recovery (e.g. as energy) and disposal.

The aim of this study was to utilize a carbon residue, which is a by-product from biomass gasification process, as a low-cost adsorbent material for water purification. Carbon residue activated chemically by zinc chloride ($ZnCl_2$) was also investigated and commercial powdered activated carbon was used as reference material. The studied metals were iron, copper and nickel. Batch experiments were done to evaluate the influence of pH, initial metal concentration and contact time. In addition, the kinetics of iron, copper and nickel were studied by the pseudo-first-order, the pseudo-second-order and the Elovich kinetic models while the adsorption mechanism was evaluated via the Weber Morris intraparticle diffusion model. The Langmuir, Freundlich and Dubinin–Radushkevich (D–R) isotherm models were also studied.

2. Materials and methods

2.1. Adsorbents

Carbon residue was obtained from a biomass gasification pilot-plant which involved a 150 kW downdraft gasifier operating at a temperature of 1000 °C. Wood chips (pine and spruce) were used as the raw material for fuel at a rate of 50 kg h^{-1}. The produced gas was washed by a wet scrubber and the carbon residue was collected from a water container. There was no separate carbon residue collector in the gasifier.

Furthermore an activated carbon residue performed by zinc chloride using a wet impregnation method was also used as an adsorbent material. Zinc chloride is one of the commonly used activating agent and also it is known to be relatively cheap chemical [29]. Powdered commercially activated carbon (pro analysis quality) provided by Merck was used as a reference sample. Before use,

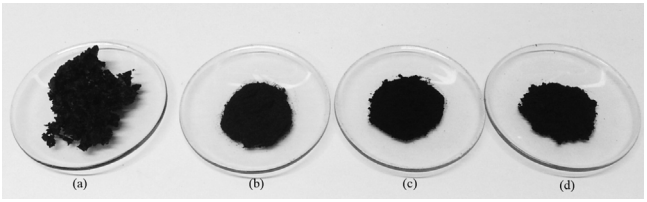

Fig. 1. Photograph of the raw material and adsorbent materials employed in this study. (a) Carbon residue (raw material) from the biomass gasification process, (b) carbon residue, (c) activated carbon residue and (d) commercial activated carbon. Adsorbent materials (b–d) used in the laboratory experiments were initially dried at 110 °C, crushed and sieved (<150 μm).

Table 2
Physical composition of adsorbents [29].

Parameter	CR	ACR	AC
Specific surface area/m^2 g^{-1}	14.4	259	603
Pore size (average)/nm	8.38	3.94	3.00
Pore volume (total)/cm^3 g^{-1}	0.03	0.26	0.45

CR: carbon residue, ACR: activated carbon residue,
AC: commercial activated carbon

all adsorbents were dried overnight at 110 °C, crushed and sieved to obtain a particle diameter less than 150 μm and to ensure a uniform product quality. In Fig. 1 an image of the raw material and adsorbent materials used in the laboratory experiments are shown. In Table 2 the physical characteristics of three adsorbent materials are presented.

2.2. Batch adsorption experiments

Adsorption of iron, copper and nickel onto different types of adsorbents was tested by using model metal solutions prepared from iron sulphate ($FeSO_4$•$7H_2O$), copper sulphate ($CuSO_4$•$5H_2O$) and nickel sulphate ($NiSO_4$•$6H_2O$). Single metal model stock solutions concentrations of 5000 mg L^{-1} were prepared by adding a metal salt to Milli-Q water and diluted further to obtain the lower concentration solution. All reagents used were of analytical reagent grade and purchased form Merck.

In the adsorption experiments, effect of adsorbent variables (pH, initial metal ion concentration and adsorption time) on the adsorption efficiency of iron, copper and nickel ions over carbon residue, activated carbon residue and commercial activated carbon were studied. To determine the optimum initial pH, batch equilibrium studies were carried at pH values of 4, 6 and 8 by using an initial concentration of 75 mg L^{-1} metal solution. pH optimization experiments were also performed without any adsorbent (zero experiment) to determine the removal of heavy metal by chemical precipitation. The initial optimum pH value for each metal was selected and adsorption experiments were performed in different initial metal concentrations (25–125 mg L^{-1}) in optimum pH. pH and concentration optimization experiments were done using polyethylene flasks of 250 mL capacity. Prior to each experiment, the metal solution (25 mL) and adsorbent material (0.125 g) were added to each flask and mixed together. The solution's pH was then adjusted by adding 0.1 M HCl and/or 0.1 M NaOH. Since carbon

residue is a strongly alkaline material and it has high buffer capacity, pH adjustment was done after adding the adsorbent to the metal solution to ensure the correct pH during adsorption experiment. Bottles were then shaken by a laboratory shaker using a reciprocating motion at a room temperature for 24 h. pH values were also measured after 24 h of adsorption experiments.

When pH and concentration optimizations were done, effect of contact time was studied in optimum conditions. Kinetic studies were performed in a 1 L reactor vessel equipped with a magnetic stirrer with an agitation speed of 1000 rpm. The volume of metal solution was 500 mL and the adsorbent dose 2.5 g. Samples (25 mL) were taken after 1 min, 2 min, 5 min, 30 min, 2 h, 4 h and 24 h reaction time. All adsorption experiments were performed at room temperature. All samples including the initial samples were filtered through 0.45 μm filter paper (Sartorius stedim biotech) and then acidified with strong nitric acid.

Heavy metals were determined in the filtrate solution by an atomic absorption spectrometer (AAS) (PerkinElmer AAnalyst 200) whose absorption wavelengths were found to be Fe (248.3 nm), Cu (324.7 nm) and Ni (232.0 nm), respectively. As an exception heavy metal concentrations from pH optimization studies were analyzed by an inductively coupled plasma optical atomic emission spectrometer (ICP-OES) (Thermo) method. The percentage removal of heavy metal (%) from the solution was calculated by the equation as follows

$$\text{Metal removal\%} = \frac{C_0 - C_e}{C_0} \times 100\% \quad (1)$$

where C_0 and C_e are the initial and equilibrium concentrations in solution (mg L^{-1}). The adsorption capacity q_e (mg g^{-1}) after equilibrium was calculated by using the following equation

$$q_e = \frac{C_0 - C_e}{m} V \quad (2)$$

where V is the volume of the solution (L) and m is the mass of the adsorbent (g) [2,30].

2.3. Effect of pH

The pH is one of the most important parameters controlling the uptake of metal ions from an aqueous solution. pH determines the surface charge of the adsorbent and the degree of ionization and speciation of the adsorbate [18]. The pH of the solution controls the electrostatic interactions between the adsorbent and the adsorbate [31]. It is known that generally the percent removal of the heavy metal ions increases with pH. At low pH, the cations compete with the H^+ ions in the solution for the sorption sites and therefore adsorption declines. In contrast as pH is increased, competition between proton and metal cation decreases which means that there are more negative groups available for the binding of metal ions which results greater metal uptake. On the other hand, at higher pH metal cations start to form hydroxide complexes or precipitate as their hydroxides which decreases the adsorption of metal ions [31–34]. In aqueous solutions metal cations hydrolyze according to the generalized expression for divalent metals as presented in Eq. (3).

$$M^{2+}(aq.) + nH_2O \leftrightharpoons M(OH)^{2-n} + nH^+ \quad (3)$$

The distribution of various hydroxo complexes depends on the pH of the solution and the corresponding stability constants. Hydroxyl-metal complexes are known to adsorb with a higher affinity than the completely hydrated metals [18].

2.4. Adsorption isotherm studies

Adsorption isotherms are generally used for the design of an adsorption system since they represent the amount of species adsorbed versus the amount of species left in the solution phase at equilibrium. The Langmuir [35] and Freundlich [36] equations are the most frequently used for describing the adsorption isotherm. The Langmuir isotherm assumes that adsorption occurs at specific homogeneous sites within the adsorbent without any interactions between the adsorbed substances. The linear form of the Langmuir isotherm model is given by a Eq. (4).

$$\frac{1}{q_e} = \frac{1}{q_m} + \frac{1}{q_m b C_e} \quad (4)$$

where q_e (mg g^{-1}) is the amount of metal ions adsorbed per unit mass of adsorbent. C_e (mg L^{-1}) is the solution concentration at equilibrium. q_m (mg g^{-1}) and b (L mg^{-1}) is the Langmuir constants related to the capacity and energy of adsorption, respectively [30]. In addition of R^2 and q_m values, the applicability of the Langmuir isotherm can be articulated by the equilibrium parameter, R_L

$$R_L = \frac{1}{1 + bC_0} \quad (5)$$

where C_0 (mg L^{-1}) is the initial concentration of the metal ion solution [37]. Langmuir isotherm considers in terms of surface coverage θ which is defined as the fraction of the adsorption sites to which a solute molecule has become attached [38]. Surface coverage θ can be obtained by a Eq. (6),

$$\theta = \frac{bC_e}{1 + bC_e} \quad (6)$$

The Freundlich model is empirical in nature and assumes that the uptake of ions occurs on a heterogeneous surface. The linear form of the Freundlich isotherm model is given by Eq. (7),

$$\log q_e = \log K_f + \frac{1}{n} \log C_e \quad (7)$$

where (L g^{-1}) and n (dimensionless) are Freundlich constants related to the adsorption capacity and intensity of adsorption, respectively [30].

In addition to Langmuir and Freundlich isotherm models, Dubinin–Radushkevich (D–R) isotherm model [39,40] is also widely used to describe adsorption process. The Dubinin–Radushkevich isotherm does not assume a homogeneous surface or constant adsorption potential. The linear form of the D–R isotherm model can be represented by the following equation:

$$\ln q_e = \ln q_m - \beta\varepsilon^2 \quad (8)$$

where q_e (mg g^{-1}) is the amount of metal ions adsorbed per unit mass of adsorbent, q_m (mg g^{-1}) is the theoretical saturation capacity, (mol^2 J^{-2}) is a constant related to the mean free energy of adsorption per mole of the metal and ε is the Polanyi potential, which is described in Eq. (9):

$$\varepsilon = RT \ln\left(1 + \frac{1}{C_e}\right) \quad (9)$$

where (J mol^{-1} K^{-1}) is the gas constant, T (K) is the absolute temperature and C_e (mg L^{-1}). By plotting $ln\ q_e$ vs. ε^2 it is possible to generate the value of q_m (mg g^{-1}) from the intercept and the value of β from the slope. The mean free energy E (kJ mol^{-1}) describes free energy change when one mole of ion is transferred from the solution to the surface of the sorbent. The mean free energy E (kJ mol^{-1}) can be calculated from the following equation:

$$E = \frac{1}{\sqrt{-2\beta}} \quad (10)$$

2.5. Adsorption kinetic studies

In order to analyze the adsorption kinetics, pseudo-first and pseudo-second-order kinetic models were applied to experimental data [30,41,42]. The first order rate equation of Lagergren is one of the most widely used for liquid adsorption studies and is expressed by the equation:

$$\log(q_e - q_t) = \log q_e - \frac{k_f}{2.303} t \quad (11)$$

where q_e and q_t are the amounts of metals adsorbed (mg g^{-1}) at equilibrium (the point at 1440 min) and at time t (min), respectively. k_f is the pseudo-first-order rate constant (min^{-1}) whilst the linear form of pseudo-second-order equation is expressed by:

$$\frac{t}{q_t} = \frac{1}{k_s q_e^2} + \frac{1}{q_e} t \quad (12)$$

where k_s is the pseudo-second-order rate equilibrium constant (g mg^{-1} min^{-1}).

The Elovich equation is initially proposed by Roginsky and Zeldowitsch [40] and has been commonly used in chemisorption processes. Elovich equation is given by the following linearized expression:

$$q = \frac{1}{\beta} \ln(\upsilon_0 \beta) + \frac{1}{\beta} \ln t \quad (13)$$

where (mg g^{-1} min^{-1}) is the initial adsorption rate and β (g mg^{-1}) is the desorption constant [33,40].

Kinetic data was analyzed using the intraparticle diffusion model on the theory proposed by Weber and Morris [43]. The amount of iron, copper and nickel adsorbed (q_t) at a particular point in time (t) was plotted against the square root of time ($t^{1/2}$), according to Eq. (14).

$$q_t = k_{id} t^{1/2} + C \quad (14)$$

where k_{id} is the intraparticle diffusion on rate determining step (mg g^{-1} min$^{-0.5}$) and C is the intercept related to the thickness of the boundary layer.

2.6. Desorption experiments

It is possible to desorb the sorbed metal from the spent adsorbent using different types of eluent agents such as distilled water, HCl, HNO_3, H_2SO_4, NaOH, CH_3COOH or EDTA solution [14,16,44–46]. In this work HCl was selected as eluent for metal desorption because it is often the most efficient eluent in many studies [14,16,45,46]. Before desorption experiment metal loaded samples were dried at 100 °C for 1 h. After that samples (0.125 g) were contacted with 25 mL of 0.1 M HCl and shaken with a magnetic stirrer at 250 rpm for 2 h at the room temperature. The desorbed metal ions were determined in the filtrate solution by AAS. Desorption efficiency can be calculated from the following equation:

$$\text{Desorption efficiency} = \frac{\text{amount of metal ions desorbed}}{\text{amount of metal ions adsorbed}} \times 100\% \quad (15)$$

3. Results and discussion

3.1. Effect of pH

Speciation diagrams were drawn for iron, copper and nickel for a concentration of 75 mg L^{-1} by using the MINEQL + software which is a chemical equilibrium modeling system [47]. As seen in Fig. 2a and b, Fe(II) ions hydrolyze to produce an array of mononuclear species, $FeOH^+$ to $Fe(OH)_3^-$, in pH values between 7 and 14. Precipitation of an insoluble ferrous hydroxide $Fe(OH)_2$ and magnetite (Fe_3O_4) occurs before any appreciable hydrolysis products are formed in the solution [48]. Ferrous ion can also be oxidized by air to ferric ions. Fe^{3+} ions hydrolyzes much more readily than Fe^{2+} ions by forming species like $FeOH^{2+}$ and $Fe(OH)_2^+$ in acidic solutions. In neutral and basic conditions $Fe(OH)_3$ and $Fe(OH)_4^-$ start to appear. The most insoluble hydroxide of ferric ion (III) is α-FeO(OH), but in the presence of ferrous ions (II) the stable phase is magnetite (Fe_3O_4) [48].

Results from the pH optimization studies (Fig. 3a) showed that at pH values 6 and 8 iron removal by precipitation is notable, over 90%. At a pH value of 4, iron removal by precipitation does not occur. To model the adsorption, authors selected pH 4 as the initial value for iron. At pH 4, the removal efficiencies for iron removal by carbon residue, activated carbon residue and commercial activated carbon were 100, 94 and 89%, respectively. To see if the pH values have remained constant during the batch experiment, the final pH values were also measured after 24 h of sorption. The final pH values for carbon residue, activated carbon residue and commercial activated carbon, after 24 h of sorption for iron removal, were 6.4, 3.2 and 3.0, respectively. Since carbon residue is clearly an alkaline material (pH ~ 9) it increases the solution's pH and because iron starts to precipitate after pH 4, it can be assumed that in the case of carbon residue, removal of iron is also based on precipitation in addition to the adsorption process, described in Eq. (3). Overall, from a utilization point of view it is insignificant how metal removal occurs, whether the mechanism is by adsorption or precipitation for example.

In Fig. 2c aqueous hydrolysis products for copper are presented by using MINEQL + software. Cu^{2+} hydrolyzes only slightly at moderate concentrations before precipitation occurs. Cu^{2+} and its hydroxo species $Cu_2(OH)_2^{2+}$ and $Cu(OH)^+$ are predominating species up to pH ~9. Hydroxo species $Cu(OH)_2$ and $Cu(OH_3)^-$ are also formed above pH ~7. In very alkaline conditions $Cu(OH)_4^{2-}$ also starts to form whilst the most insoluble phase of Cu^{2+} is CuO [32,48,49].

Results from pH optimizations experiments showed that copper does not precipitate at pH 4. The removal efficiency for copper by precipitation is about 10% at pH 6 whereas at pH 8 copper removal is based solely on the precipitation process. To investigate adsorption capacity the authors decided to select pH 5 as the initial value for copper. Rozaini et al. [34] also selected pH 5 for the optimum pH for Cu(II) removal, because $Cu(OH)_2$ (s) are the dominant species at pH greater than 6. When pH optimization experiments were performed at the initial pH value 4, the final pH values for carbon residue, activated carbon residue and commercial activated carbon were 5.1, 5.4 and 5.2, respectively. Therefore it can be assumed that the removal of copper by different adsorbent materials is based on the precipitation process in addition to adsorption also at the initial pH 5. As seen in Fig. 3b the removal efficiencies for copper by carbon residue, activated carbon residue and commercial activated carbon were 68, 100 and 25%, respectively at pH 5.

As seen in Fig. 2d depending on the pH of the system, nickel(II) can exist as Ni^{2+}, $Ni(OH)^+$, $Ni(OH)_2$ and $Ni(OH)_3^-$. At higher pH values, especially greater than 7.5, the amount of sorption sharply decreases due to the formation of $Ni(OH)_2$ (s), which tends to precipitate at higher pH values [48–50].

Ewecharoen et al. [51] noticed that at pH higher than 7.7 nickel starts to precipitate due to the formation of $Ni(OH)_2$. On the other hand Rozaini et al. [34] and Hasar [52] noticed that precipitate already starts when the pH value exceeds 5. The authors selected pH 8 as the optimum initial pH value for nickel. Results show that at initial pH 8 the removal efficiencies for nickel by carbon residue, activated carbon residue and commercial activated carbon were 46, 86 and 28%, respectively (Fig. 3c). Nickel removal by precipitation is about 10% at initial pH 8. The final pH values after 24 h batch

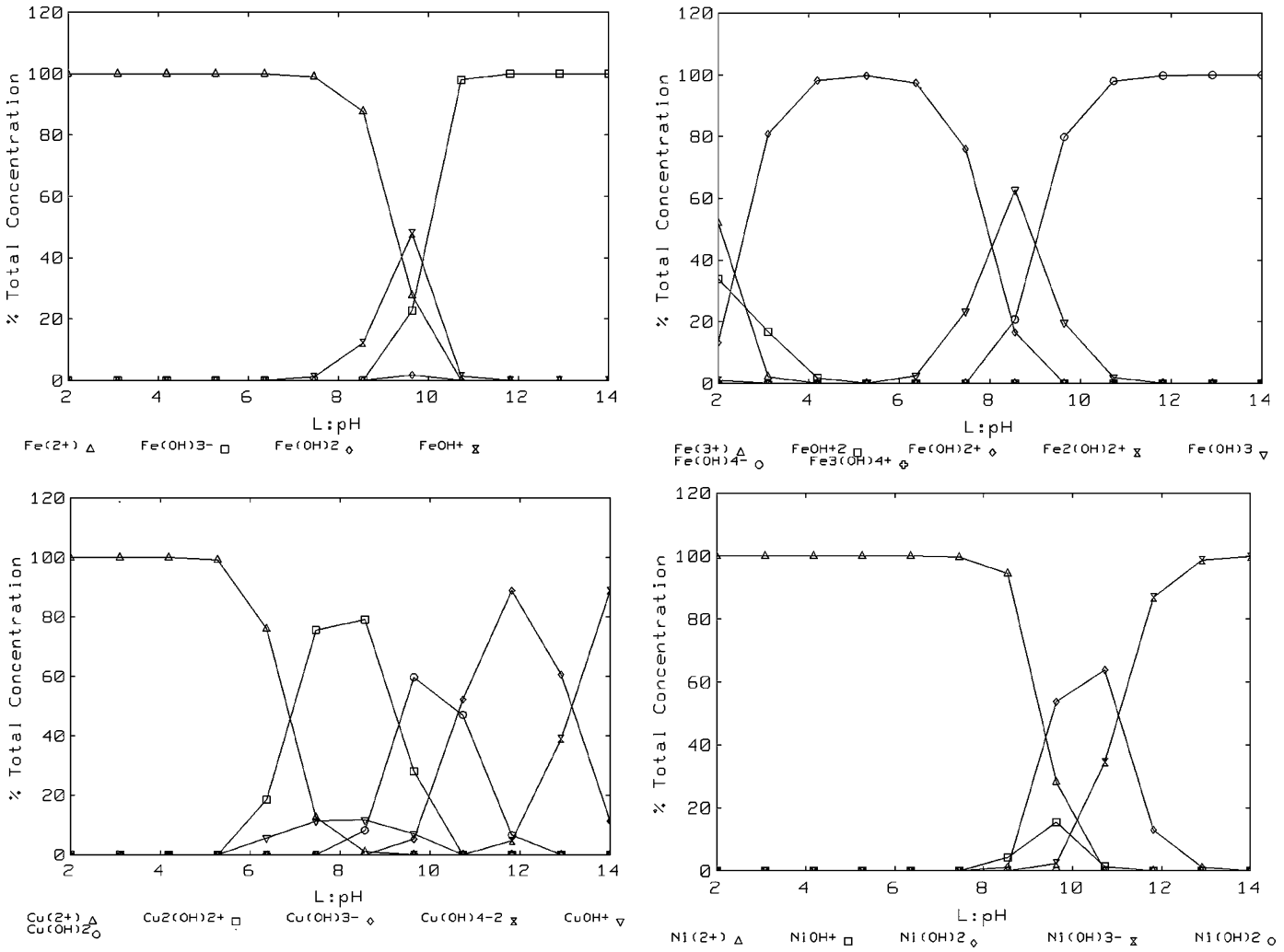

Fig. 2. (a) Fe(II), (b) Fe(III), (c) Cu(II) and (d) Ni(II) soluble hydrolysis products presented as total concentration as a function of pH in liquid phase. Metal concentration 75 mg L^{-1}.

adsorption experiments were 8.0, 6.9 and 7.3 for carbon residue, activated carbon residue and commercial activated carbon, respectively.

3.2. Effect of initial metal concentration

Experimental results for the removal of iron, copper and nickel ions on the different types of adsorbents in the metal concentration range of 25–125 mg L^{-1} at the optimum initial pH for each metal are shown in Fig. 4.

Results show that in the case of copper and nickel removal by carbon residue, sorption capacity q_e initially rises sharply, indicating that specific adsorption sites are available for adsorption of the metal ions. At higher initial metal concentrations the adsorbent becomes saturated and no more sites are available for further sorption. For the commercial activated carbon, the same phenomenon deals with all the studied metals. Activated carbon residue displayed high removal efficiency (100%) toward copper for the concentration range 25–125 mg L^{-1} and iron and nickel removal was also very high. The maximum sorption capacities ($q_{m,\exp}$) for iron, copper and nickel by activated carbon residue were 20.5, 23.1 and 18.2 mg g^{-1}, respectively. Carbon residue displayed a 100% removal efficiency toward iron for the concentration range 25–125 mg L^{-1} and the removal efficiency was better than that of the commercial activated carbon for all metals. Corresponding values without activation were (Fe(II): 24.1, Cu(II): 11.1 and Ni: 5.6 mg g^{-1}). The maximum sorption capacity of commercial activated carbon for iron, copper and nickel were 13.9, 5.1 and 2.9 mg g^{-1}, respectively. The optimum initial metal concentrations for carbon residue, activated carbon residue and commercial activated carbon were selected: 125, 25 and 25 mg L^{-1} for iron, 25, 100, 25 mg L^{-1} for copper and 25, 125 and 25 mg L^{-1} for nickel, respectively. In all concentration optimization experiments metal precipitation cannot be totally neglected.

Both activated carbon residue and carbon residue turned out to be better adsorbent materials than commercial activated carbon. This might be due to carbon residue and activated carbon residue possessing different kinds of components (nutrients and heavy metals), which makes their surface a better adsorbent material. For example, carbon residue includes a notable amount of calcium (42.3 g kg^{-1}). Also carbon residue includes potassium (2.3 g kg^{-1}), magnesium (3.2 g kg^{-1}), sodium (71 mg kg^{-1}), copper (<10.1 mg kg^{-1}) and zinc (66.1 mg kg^{-1}) [53]. Carbon residues from the gasification process have typically lower specific surface area compared with commercial activated carbon but its carbon content is usually high [29]. Chemical activation also can increase the surface area and pore volume of adsorbent [54]. As can be seen in Table 2 specific surface area, pore size and volume are bigger for activated carbon residue than non-activated carbon residue. This can be explained by the fact that cavities are also formed in

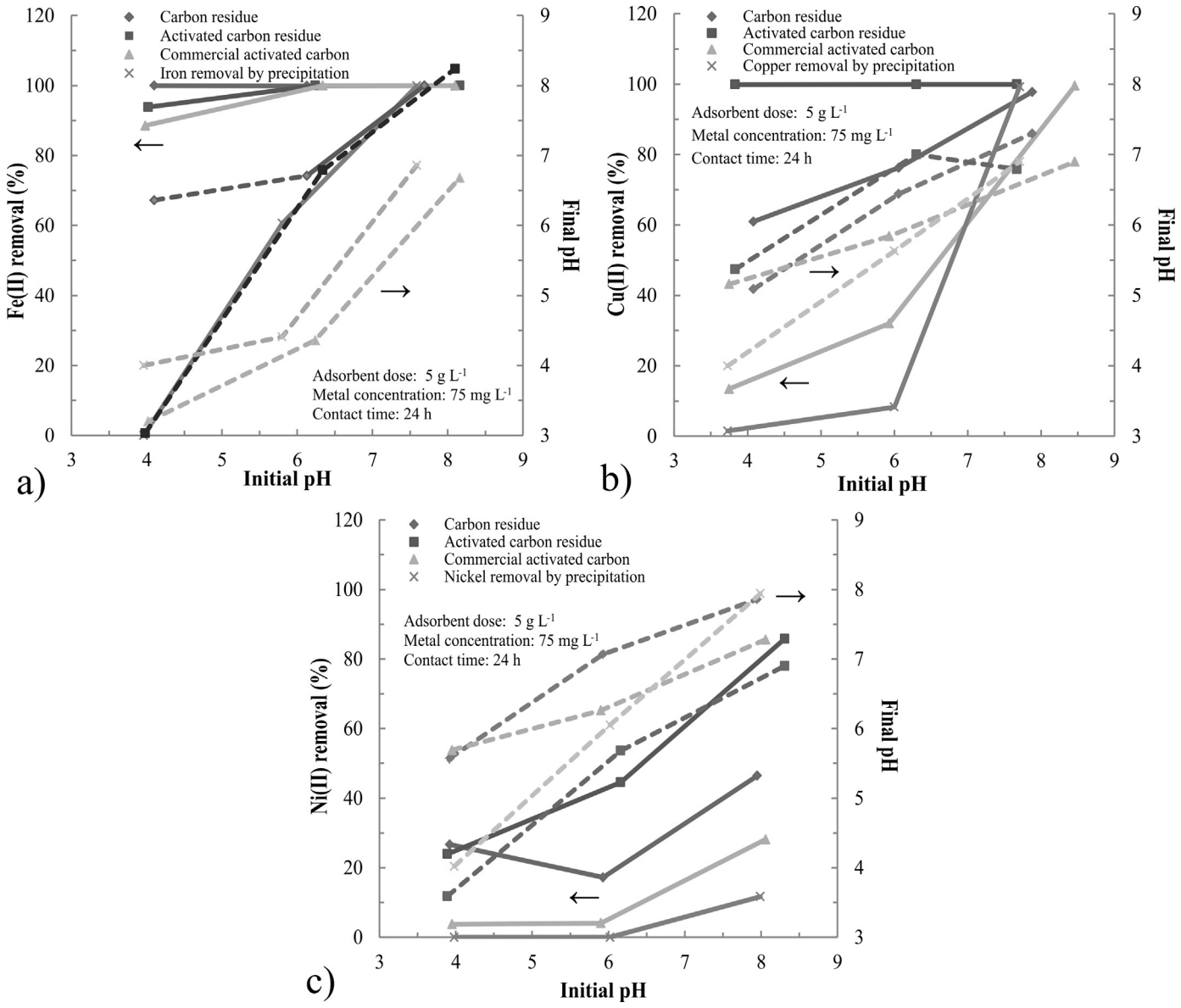

Fig. 3. Effect of initial pH on the adsorption of (a) iron, (b) copper and (c) nickel onto different types of adsorbents. Dashed lines corresponds to the equality of initial and final pH. Experiments were also used without adsorbent (x) to determine studied cations removal by precipitation.

the activation step due to the evaporation of zinc chloride which increases the specific surface area [55].

Adsorption potential of carbon residue with and without chemical activation as a low cost adsorbent from the present study was compared with other adsorbents reported in other studies (Table 3). It is seen that studied adsorbents shows comparable adsorption capacity for iron, copper and nickel removal.

3.3. Adsorption isotherms

The constants of Langmuir, Freundlich and Dubinin–Raduschkevich (D–R) isotherm are obtained from the linear plots of $1/q_e$ versus $1/C_e$, $\log q_e$ versus $\log C_e$ and $\ln q_e$ versus ε^2, respectively (Table 4). We have not presented Langmuir, Freundlich and D–R constants for the removal of iron by carbon residue and copper by activated carbon residue since the 100% removal efficiency for the whole concentration range 25–125 mg L^{-1} (see Fig. 4a and b).

The correlation coefficients, values of R^2 are regarded as a measure of the goodness-of-fit for experimental data (by the isotherm's models). According to these values sorption of studied metals by activated carbon residue fitted better to Langmuir than Freundlich and D–R isotherm models. This was also the case in the removal of copper and nickel by commercial activated carbon whilst Freundlich isotherm gave better R^2 value than Langmuir and D–R models in the case of iron removal. In the case of carbon residue Freundlich model gives slightly better values of R^2 than Langmuir and D–R models. The Freundlich parameter $1/n$ is between 0.1 and 1 indicating that the sorption is favorable [66].

It is seen from Table 4 that experimentally obtained values of $q_{m,exp}$ are comparable to the maximum sorption obtained from the Langmuir adsorption isotherm (q_m). This suggests the monolayer coverage of metal ions onto different types of adsorbents. In the case of nickel removal by activated carbon the maximum sorption capacity (q_m) is found to be 62.9 mg g^{-1} which is higher than the experimental value ($q_{m,exp}$) 18.2 mg g^{-1}. This may be a consequence

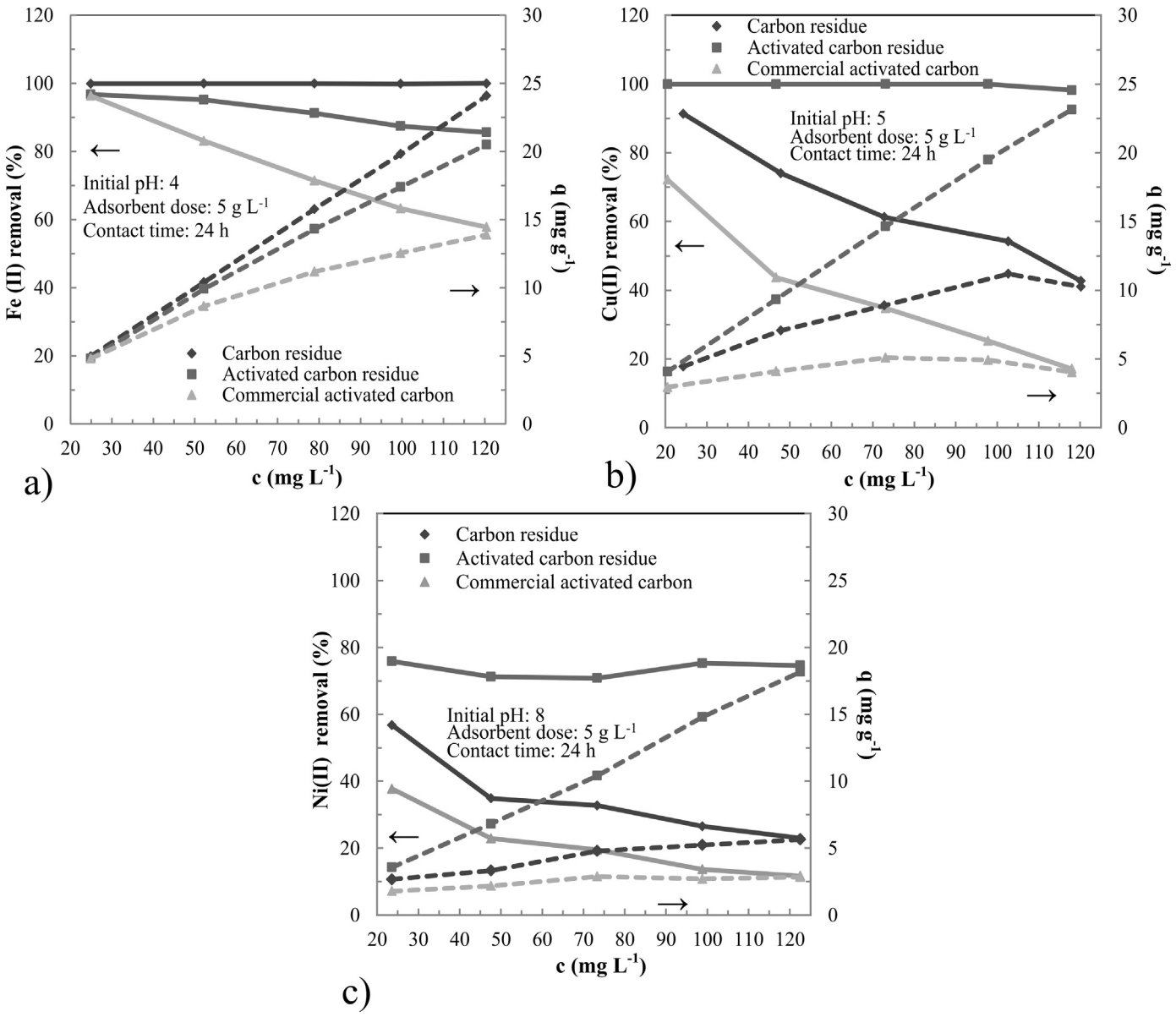

Fig. 4. Effect of initial metal concentration on the removal efficiency of (a) iron, (b) copper and (c) nickel onto different types of adsorbents.

of the fact that nickel removal is very high (~71–76%) at whole concentration range 25–125 mg L^{-1} and therefore maximum metal uptake could not be reached in the experiments (Fig. 4c). Langmuir parameter R_L indicates the feasibility of the adsorption process: the adsorption process is unfavorable if $R_L > 1$, linear when $R_L = 1$, favorable in the range $0 < R_L < 1$ or irreversible ($R_L = 0$). Based on the results, R_L values lie between 0 and 1 for studied metals suggesting that the Langmuir model is favorable for all adsorbents (Table 5). Furthermore, higher R_L values at lower metal concentrations show that the adsorption is more favorable at lower metal concentrations [37,66,67]. Surface coverages (θ) are also presented in the Table 5.

D–R parameter, the mean free energy E (kJ mol^{-1}), gives idea about the type of adsorption mechanism as chemical ion-exchange or physical adsorption. The magnitude of E between 8 and 16 kJ mol^{-1} corresponds to a chemical ion-exchange process. If the E is less than 8 kJ mol^{-1}, the adsorption is physical in nature [68]. Results (Table 4) show that E values are lower than 8 kJ mol^{-1} in all studied adsorbate–adsorbent systems. This indicates that the sorption process may be a physical in nature.

3.4. Effect of contact time and kinetic modeling

The adsorption of metals (Fe, Cu and Ni) on three different adsorbent materials was studied as a function of adsorption time (1 min – 24 h) with an initial optimum pH and metal concentrations. Corresponding results are showed in Fig. 5. In all cases the rate of percent metal removal is higher in the beginning of adsorption experiment due to a larger surface area of the adsorbent being available for the adsorption of metals [33]. The activated carbon residue is the best adsorbent for all the metals. The removal efficiency of iron and copper ions by that increases with time and attains saturation in about 120 min. For nickel, the removal rate is very fast. The best removal efficiency is achieved in about 1 min but after that the removal efficiency starts to decrease gradually. This can be explained by a decrease in the initial pH value of 8.1 to a pH value of 7.1 (after 24 h reaction time). Therefore it is possible that at a higher pH value nickel removal is based on precipitation, in addition to adsorption causing better removal efficiency toward nickel. The carbon residue shows also good removal efficiency especially toward copper and nickel. In the case of carbon residue maximum

Table 3
Comparison of maximum sorption capacities for copper and nickel (mg g^{-1}).

Metal	Adsorbent	Adsorption capacity q(mg g^{-1})	References
Iron			
	Cow bone charcoal[b]	31.4	[56]
	Commercial activated carbon[b]	31.0	[57]
	Carbon residue from biogasification process[a]	24.1	This study
	Chemically ($ZnCl_2$) activated carbon residue[a]	20.5	This study
	Commercial activated carbon (powered)[a]	13.9	This study
	Hazelnut hull[b]	13.6	[58]
Copper			
	Granular biomass[a]	55.0	[59]
	Cow bone charcoal[b]	35.4	[56]
	Chemically ($ZnCl_2$) activated carbon residue[a]	23.1	This study
	Activated carbon produced from pomegranate peel[b]	18.1–22.0	[33]
	Coal fly ash pellets[b]	20.9	[60]
	Red mud[b]	19.7	[61]
	Na-Bentonite[b]	17.9	[23]
	Carbon residue from biogasification process[a]	10.3	This study
	H_3PO_4-activated rubber wood sawdust[b]	5.7	[62]
	Commercial activated carbon (powered)[a]	5.1	This study
	Bagasse fly ash[b]	2.3	[63]
	Olive stone waste[b]	1.9	[14]
Nickel			
	Irradiation-grafted activated carbon[b]	55.7	[51]
	Cow bone charcoal[b]	32.5	[56]
	Activated carbon prepared from almond husk[b]	30.8–37.2	[52]
	Granular biomass[a]	26.0	[59]
	Chemically ($ZnCl_2$) activated carbon residue[a]	18.2	This study
	Activated carbon from *Hevea brasiliensis*[b]	17.2	[64]
	Coir pith waste[b]	16.0	[65]
	Na-bentonite[b]	14.0	[23]
	Red mud[b]	11.0	[61]
	Carbon residue from biogasification process[a]	5.6	This study
	Commercial activated carbon (powered)[a]	2.9	This study
	Olive stone waste[b]	2.1	[14]

[a] Experimental value $q_{m,\exp}$.
[b] Langmuir parameter q_m.

uptake is not achieved during adsorption experiment (24 h). The same trend is in the case of removal iron and copper by activated carbon. Especially in the case of carbon residue this phenomena can be explained by the fact that carbon residue as an alkaline material (pH ~ 9) increases the solution's pH and metal starts to precipitate in addition of adsorption increasing total removal efficiency during adsorption experiment.

Results showed that the correlation coefficients for the pseudo-first-order and the Elovich kinetic models were less than 0.99. In addition, experimental uptake values ($q_{e(\exp)}$) were not reasonable fit in regard to the calculated values ($q_{e(\mathrm{cal})}$). Therefore pseudo-second-order kinetic model was selected to be the best-fit model and only results from pseudo-second-order kinetics studies are presented (Table 6 and Fig. 6).

In all cases the experimental $q_{e(\exp)}$ correspond to calculated $q_{e(\mathrm{cal})}$ values. Furthermore, linear regression values (R^2) are higher than 0.99 indicating that the kinetics of sorption can be described well by the pseudo-second-order equation. In the case of nickel removal by activated carbon residue the calculated rate constant is negative and is not included in Table 6. The negative rate constant can be explained by the fact that the maximal nickel removal efficiency was achieved in 1 min but then starts to decrease with time as presented in Fig. 5c. In the case of copper removal by activated carbon residue we do not have a result for the copper removal efficiency after 24 h so we have used the result from concentration optimization experiments after 24 h instead.

Comparison of removal efficiencies (%) and experimental uptake values (mg g^{-1}) from concentration optimization experiments

Table 4
Constants of Langmuir, Freundlich and Dubinin–Raduschkevich isotherms.

Adsorbent	Adsorbate	$q_{m,\exp}$ (mg g^{-1})	Langmuir isotherm parameters			Freundlich isotherm parameters			D–R isotherm parameters		
			q_m (mg g^{-1})	b (L mg^{-1})	R^2	K_f (L g^{-1})	$1/n$	R^2	q_m (mg g^{-1})	E (kJ mol^{-1})	R^2
CR	Fe	24.1	25.4	–	–	–	–	–	26.0	–	–
	Cu	11.1	10.1	0.37	0.9439	3.71	0.2602	0.9704	9.3	0.78	0.8120
	Ni	5.6	5.7	0.08	0.8610	1.12	0.3544	0.9417	4.8	0.20	0.6916
ACR	Fe	20.5	21.4	0.36	0.9968	5.77	0.4547	0.9805	16.2	1.24	0.8871
	Cu	23.1	23.3	–	–	–	–	–	23.3	–	–
	Ni	18.2	62.9	0.01	0.9797	0.63	0.9579	0.9696	13.6	0.23	0.7895
AC	Fe	13.9	12.1	0.72	0.9517	4.92	0.2626	0.9998	11.5	1.37	0.8412
	Cu	5.1	4.4	0.22	0.8406	2.39	0.1546	0.6420	4.6	0.42	0.7788
	Ni	2.9	3.1	0.09	0.9118	0.93	0.2493	0.8879	2.7	0.17	0.8065

CR: carbon residue, ACR: activated carbon residue, AC: commercial activated carbon.

Table 5
R_L values and surface coverages (θ) for the different adsorbent types at different concentrations of metal ions.

Adsorbent	C_0 (mg L^{-1})	R_L			θ		
		Fe(II)	Cu(II)	Ni(II)	Fe(II)	Cu(II)	Ni(II)
CR	25	–	0.0999	0.3452	–	0.44	0.45
	50	–	0.0534	0.2072	–	0.82	0.71
	75	–	0.0357	0.1451	–	0.91	0.80
	100	–	0.0256	0.1119	–	0.95	0.85
	125	–	0.0220	0.0922	–	0.96	0.88
ACR	25	0.1004	–	0.8039	0.22	–	0.06
	50	0.0505	–	0.6702	0.47	–	0.12
	75	0.0340	–	0.5689	0.71	–	0.18
	100	0.0271	–	0.4947	0.82	–	0.20
	125	0.0226	–	0.4413	0.86	–	0.24
AC	25	0.0526	0.1491	0.3228	0.39	0.61	0.57
	50	0.0258	0.0714	0.1912	0.86	0.88	0.77
	75	0.0172	0.0468	0.1331	0.94	0.93	0.84
	100	0.0137	0.0354	0.1022	0.96	0.95	0.88
	125	0.0114	0.0295	0.0841	0.97	0.96	0.91

CR: carbon residue, ACR: activated carbon residue, AC: commercial activated carbon.

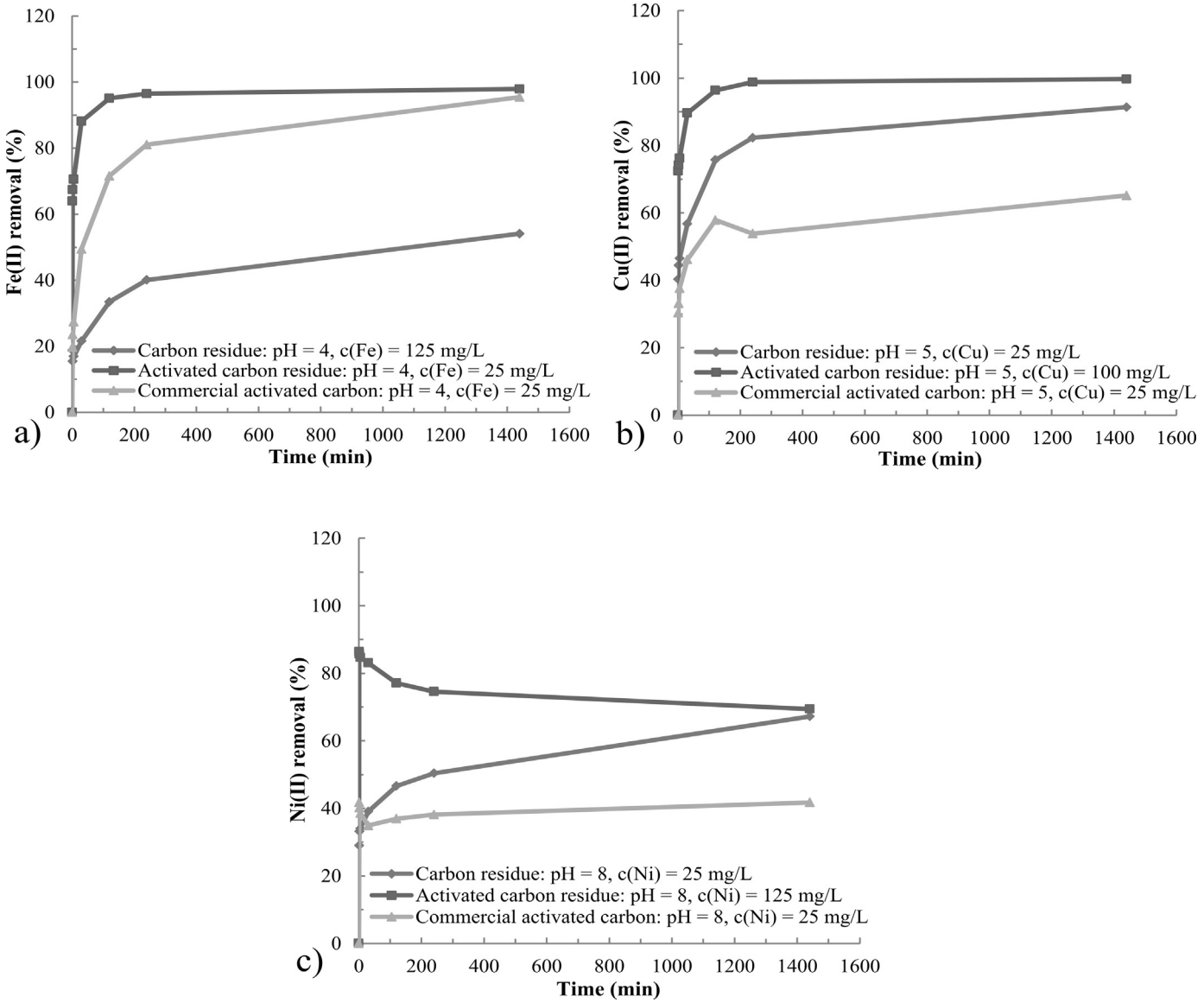

Fig. 5. Effect of contact time on the removal efficiency of (a) iron, (b) copper and (c) nickel onto different types of adsorbents at optimum initial pH and metal concentrations for each metal.

Table 6
Removal efficiencies and pseudo-second-order kinetic model parameters for different adsorbents in iron, copper and nickel experiments.

Adsorbent	Metal	Initial pH	C_0 (mg L^{-1})	Removal (24 h) %	$q_{e(exp)}$ (mg g^{-1})	$q_{e(cal)}$ (mg g^{-1})	k_s (g mg^{-1} min^{-1})	R^2
CR	Fe	4	125	54.1	16.6	16.9	0.0016	0.9955
	Cu	5	25	91.4	4.4	4.5	0.0175	0.9996
	Ni	8	25	67.2	3.2	3.2	0.0119	0.9965
ACR	Fe	4	25	97.9	5.6	5.6	0.0772	0.9999
	Cu	5	100	99.7	20.2	20.2	0.0236	0.9999
	Ni	8	125	69.4	15.3	15.3	–	0.9998
AC	Fe	4	25	95.4	5.4	5.5	0.0082	0.9990
	Cu[a]	5	25	65.2	3.2	3.2	0.0231	0.9989
	Ni	8	25	41.8	2.1	2.1	0.0677	0.9997

CR: carbon residue, ACR: activated carbon residue, AC: commercial activated carbon.
Where q_e is the amount of iron, copper or nickel adsorbed on adsorbent (mg g^{-1}) at equilibrium; k_s is the rate constant for pseudo-second-order kinetics (g mg^{-1} min^{-1}) while R^2 is the linear correlation coefficient. Number of points was 7.
[a]The last experimental result (the result for 24 h) is from concentration optimization experiments.

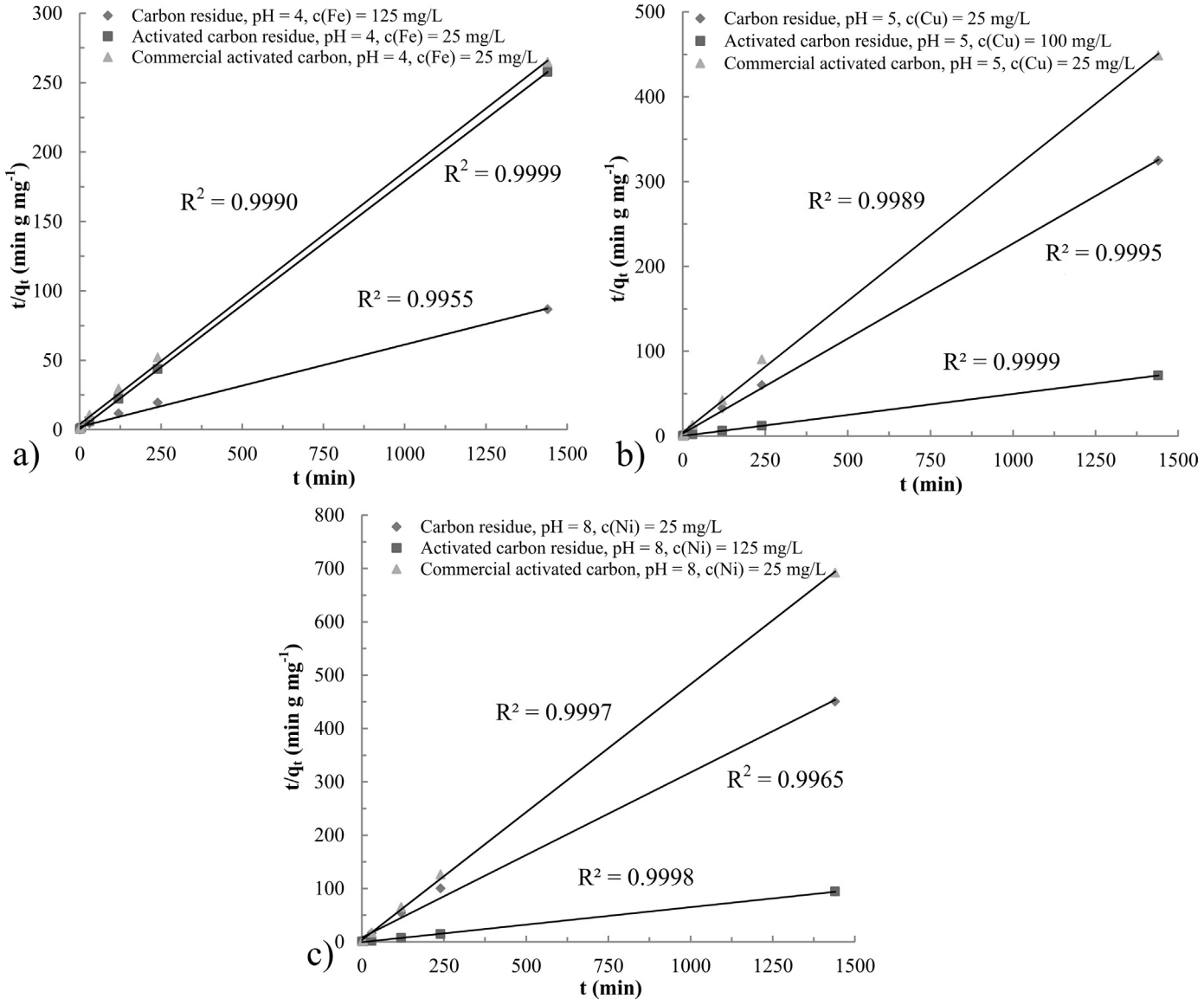

Fig. 6. Pseudo-second-order kinetic plots of adsorption of (a) iron, (b) copper and (c) nickel on carbon residue, activated carbon residue and commercial activated carbon at the optimum initial pH and metal concentration.

(Fig. 4) and kinetic studies (Fig. 5 and Table 6) at the corresponding conditions, shows that values are quite similar. Small differences in values can be explained by variances in pH levels during the experiment. The biggest difference between these values is in the case of iron removal by carbon residue. Corresponding maximum experimental uptake values are 24.1 mg g^{-1} and 16.6 mg g^{-1} from the concentration optimization experiment and from kinetic studies, respectively. The difference can be explained due to a lower pH of

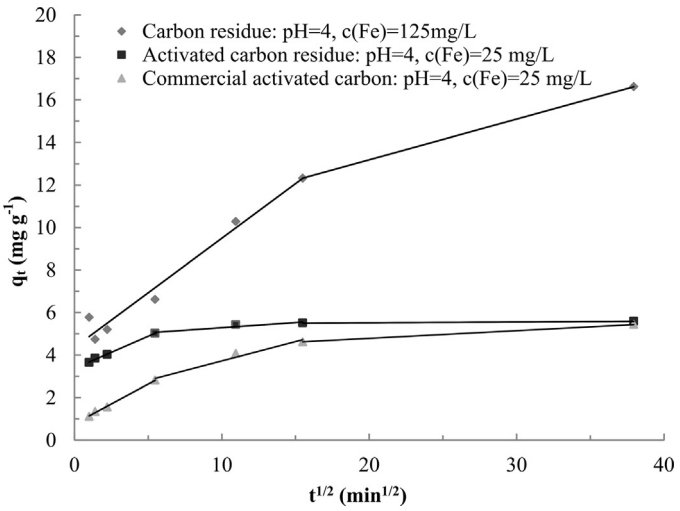

Fig. 7. Weber and Morris intraparticle diffusion model plots of iron adsorption on carbon residue, activated carbon residue and commercial activated carbon.

the solution during kinetic studies than during the concentration optimization experiment. The last pH adjustment (pH 4) was done after 32 min reaction time during kinetic studies and therefore, the pH value might have been lower during kinetic studies than during concentration optimization experiments. So it can be assumed that iron removal is based more on adsorption in the case of kinetics studies than for concentration optimization studies. However, iron removal by precipitation cannot be totally neglected even in kinetic studies.

3.5. Weber and Morris intraparticle diffusion model

If the adsorption mechanism only follows the intraparticle diffusion process, a plot of q_t versus $t^{1/2}$ should be a straight line from the origin. If the data exhibits multi-linear plots, then the process is governed by two or more steps. As can be seen in Fig. 7, the data of iron sorption on all the adsorbents exhibits multi-linear plots (two or three plots) and plots do not pass through the origin. Also in the case of copper removal by all adsorbents and nickel removal by carbon residue the same phenomena was observed (not shown here). The first stage can be attributed to the instantaneous or external surface adsorption, for example the diffusion of the metal ions through the solution to the external surface of the adsorbent. The second stage can be attributed to the slow diffusion of metal ions from the surface sites into inner pores, where intra-particle diffusion can be assumed as a rate-controlling step. In the third stage intra-particle diffusion starts to slow down due to low metal ion concentrations left in the solution [30,33,69–71]. In the case of nickel removal by activated carbon residue and commercial activated carbon, the authors not applied the intraparticle diffusion model because the best removal efficiency was achieved already at the begin of the adsorption experiment (see Fig. 5c). However, all adsorbents exhibit two or three plots for all studied metals and plots do not pass through the origin.

3.6. Desorption experiments

Desorption experiments were done by treating metal loaded adsorbent materials with 0.01 M HCl. As can be seen in Table 7 desorption efficiencies are high for all studied adsorbate–adsorbent systems. One possible explanation for high desorption efficiencies can be formation of chloro-complexes when HCl reacts with metal ions [14]. The lowest sorption efficiency (79.4%) was achieved in the case of copper desorption from activated carbon residue. In the case of carbon residue for all studied metals and activated carbon residue for iron and nickel desorption efficiencies are higher than 100%. This can be explained by the fact that carbon residue as a industrial by-product includes many metals such as iron, copper and nickel which start also to dissolve to solvent [53]. Due to high desorption efficiencies for all studied adsorbate–adsorbent systems it can be assumed that sorption process is reversible in nature.

3.7. Adsorption mechanism

It is quite difficult to evaluate the adsorption mechanism by which the Fe(II), Cu(II) and Ni(II) metal ions are adsorbed onto to our samples because formed by-product includes many metals and compounds which can affect on adsorption process [53]. According to Dias et al. [72] the predominant interactions in the metal adsorption process on activated carbon are of electrostatic nature because metallic species have small size and they are frequently charged in solution. The factors that mainly control the extent of adsorption process on activated carbon are (1) the chemistry of the metal ion (speciation) or metal ion complex, (2) the solution pH and the point of zero charge of the surface, (3) the surface area and porosity (narrow and wider microporosity), (4) the surface composition (oxygen functionality) and (5) the size of adsorbing species. According to Ahmaruzzaman [1] in the case of the various industrial adsorbents the adsorption mechanisms can be very complicated and appear attributable to electrostatic attraction, ion-exchange, adsorption–precipitation, hydrogen bonding, and chemical interaction between metal ions and the surface functional groups of the various industrial adsorbents.

Our results showed that the mean free energy E (kJ mol^{-1}) was below 8 kJ mol^{-1} and desorption efficiency was high for all studied adsorbate–adsorbent systems. Based on our preliminary IR studies our samples do not include functional groups. Specific surface area, pore size and pore volume are important physical properties in adsorption process. Differences in the surface area and porosity of particles within a material can affect its performance characteristics. By chemical activation it is possible to develop the porosity of adsorbent material (by means of dehydratation and degradation). Due to the chemical activation zinc chloride activated carbon can

Table 7
Adsorption and desorption data for Fe(II), Cu(II) and Ni(II) onto different types of adsorbents.

Adsorbent	Metal	Adsorption, 1 h (mg g^{-1})	Desorption, 2 h (mg g^{-1})	Desorption efficiency, 2 h (%)
CR	Fe	16.8	19.7	117.3
	Cu	4.2	4.8	114.3
	Ni	2.4	3.7	154.2
ACR	Fe	5.9	7.2	122.0
	Cu	16.5	13.1	79.4
	Ni	13.8	15.0	108.7
AC	Fe	3.8	3.6	94.7
	Cu	3.1	2.9	93.5
	Ni	2.5	2.7	108.0

CR: carbon residue, ACR: activated carbon residue, AC: commercial activated carbon.

be more effective adsorbent material than carbon residue and commercial activated carbon for removal of metal ions. According to the results it can be assumed that sorption process is physical and reversible in nature and could be based on the porosity of material. In our studies especially in the case of carbon residue it is obvious that metal removal is based on metal precipitation as hydroxides in addition of adsorption. It is also worth mentioning that from the utilization point of view it is insignificant if the metal removal occur via adsorption or via precipitation.

4. Conclusions

The results from the present study exhibit the potential of carbon residue for iron, copper and nickel removal from aqueous solutions. The optimum pH required for maximum adsorption was found to be 4, 5 and 8, for iron, copper and nickel, respectively. The maximum sorption capacities ($q_{m,\mathrm{exp}}$) for iron, copper and nickel by activated carbon residue were 20.5, 23.1 and 18.2 mg g^{-1}, respectively at room temperature. Corresponding values without activation were (Fe(II): 24.1, Cu(II): 11.1 and Ni: 5.6 mg g^{-1}) at room temperature. Especially the activated ($ZnCl_2$) carbon residue but also the carbon residue without activation showed better removal efficiency for iron, copper and nickel than commercial activated carbon at the concentration range of 25–125 mg L^{-1}. The maximum sorption capacity of commercial activated carbon for iron, copper and nickel were 13.9, 5.1 and 2.9 mg g^{-1}, respectively. Sorption kinetics followed the pseudo-second-order kinetic model whilst the Weber and Morris intraparticle diffusion model showed that the sorption mechanism included two or three different steps depending on adsorbate. Adsorption isotherm studies indicated that Langmuir model fitted well for iron, copper and nickel adsorption onto activated carbon residue. Results indicate that the carbon residue with and without chemical activation is an efficient adsorbent and thus carbon residues formed in the gasification process could be utilized in wastewater treatment.

Acknowledgments

This study has been undertaken with the financial support Maaja vesitekniikan tuki ry. within the project Moniwater. The authors are grateful to B.Sc. (Chem) Terhi Kolehmainen for her contribution in conducting the experiments. The authors would also like to thank Mr. Jaakko Pulkkinen and Suomen Ympäristöpalvelu Oy laboratory staff for their help in metal analysis.

References

[1] M. Ahmaruzzaman, Industrial wastes as low-cost potential adsorbents for the treatment of wastewater laden with heavy metals, Adv. Colloid Interface Sci. 166 (2011) 36–59.
[2] A.K. Meena, G.K. Mishra, P.K. Rai, C. Rajagopal, P.N. Nagar, Removal of heavy metal ions from aqueous solutions using carbon aerogel as an adsorbent, J. Hazard. Mater. 122 (2005) 161–170.
[3] Helcom recommendation 20E/6 requirements for discharging of waste water from the chemical industry, 2014, http://helcom.fi/recommendations/rec%2016-7.pdf (accessed 21.03.14).
[4] Lenntech, Drinking water standards, 21.3 (2014), Available from: http://www.lenntech.com/applications/drinking/standards/drinking-water-standards.htm
[5] US EPA, National Primary Drinking Water Regulations (1995), Available from: http://water.epa.gov/drink/contaminants/index.cfm (accessed 21.03.14).
[6] Global Drinking, Water Quality Index Development and Sensitivity Analysis Report (2007), Available from: http://www.un.org/waterforlifedecade/pdf/global_drinking_water_quality_index.pdf (accessed 21.03.14).
[7] J. Kim, M.M. Benjamin, Modeling a novel ion exchange process for arsenic and nitrate removal, Water Res. 38 (2004) 2053–2062.
[8] J.O. Esalah, M.E. Weber, J.H. Vera, Removal of lead, cadmium and zinc from aqueous solutions by precipitation with sodium di-(*n*-octyl) phosphinate, Can. J. Chem. Eng. 78 (2000) 948–954.
[9] E. Samper, M. Rodríguez, M.A. De la Rubia, D. Prats, Removal of metal ions at low concentration by micellar-enhanced ultrafiltration (MEUF) using sodium dodecyl sulfate (SDS) and linear alkylbenzene sulfonate (LAS), Sep. Purif. Technol. 65 (2009) 337–342.
[10] M. Mohsen-Nia, P. Montazeri, H. Modarress, Removal of Cu^{2+} and Ni^{2+} from wastewater with a chelating agent and reverse osmosis processes, Desalination 217 (2007) 276–281.
[11] Z. Yu, W. Admassu, Modeling of electrodialysis of metal ion removal from pulp and paper mill process stream, Chem. Eng. Sci. 55 (2000) 4629–4641.
[12] L. Fischer, T. Falta, G. Koellensperger, A. Stojanovic, D. Kogelnig, M. Galanski, R. Krachler, B.K. Keppler, S. Hann, Ionic liquids for extraction of metals and metal containing compounds from communal and industrial waste water, Water Res. 45 (2011) 4601–4614.
[13] H. Polat, D. Erdogan, Heavy metal removal from waste waters by ion flotation, J. Hazard. Mater. 148 (2007) 267–273.
[14] N. Fiol, I. Villaescusa, M. Martínez, N. Miralles, J. Poch, J. Serarols, Sorption of Pb(II), Ni(II), Cu(II) and Cd(II) from aqueous solution by olive stone waste, Sep. Purif. Technol. 50 (2006) 132–140.
[15] F. Pagnanelli, S. Mainelli, F. Vegliò, L. Toro, Heavy metal removal by olive pomace: biosorbent characterisation and equilibrium modelling, Chem. Eng. Sci. 58 (2003) 4709–4717.
[16] N. Sharma, K. Kaur, S. Kaur, Kinetic and equilibrium studies on the removal of Cd^{2+} ions from water using polyacrylamide grafted rice (*Oryza sativa*) husk and (*Tectona grandis*) saw dust, J. Hazard. Mater. 163 (2009) 1338–1344.
[17] C. Zhu, L. Wang, W. Chen, Removal of Cu(II) from aqueous solution by agricultural by-product: peanut hull, J. Hazard. Mater. 168 (2009) 739–746.
[18] H. Cho, D. Oh, K. Kim, A study on removal characteristics of heavy metals from aqueous solution by fly ash, J. Hazard. Mater. 127 (2005) 187–195.
[19] S.M. Lee, A.P. Davis, Removal of Cu(II) and Cd(II) from aqueous solution by seafood processing waste sludge, Water Res. 35 (2001) 534–540.
[20] H. Nadaroglu, E. Kalkan, N. Demir, Removal of copper from aqueous solution using red mud, Desalination 251 (2010) 90–95.
[21] J. Lakatos, S.D. Brown, C.E. Snape, Coals as sorbents for the removal and reduction of hexavalent chromium from aqueous waste streams, Fuel 81 (2002) 691–698.
[22] Ö. Yavuz, Y. Altunkaynak, F. Güzel, Removal of copper, nickel, cobalt and manganese from aqueous solution by kaolinite, Water Res. 37 (2003) 948–952.
[23] Z. Liu, S. Zhou, Adsorption of copper and nickel on Na-bentonite, Process Saf. Environ. Prot. 88 (2010) 62–66.
[24] A. Bhatnagar, M. Sillanpää, Utilization of agro-industrial and municipal waste materials as potential adsorbents for water treatment – a review, Chem. Eng. J. 157 (2010) 277–296.
[25] G. Berndes, M. Hoogwijk, R. van den Broek, The contribution of biomass in the future global energy supply: a review of 17 studies, Biomass Bioenergy 25 (2003) 1–28.
[26] H.A.M. Knoef, Handbook Biomass Gasification, BTG Biomass Technology Group BV, The Netherlands, 2005.
[27] P. McKendry, Energy production from biomass (part 3): gasification technologies, Bioresour. Technol. 83 (2002) 55–63.
[28] Directive 2008/98/EC of the European parliament and of the council, Official Journal of the European Union (2008) (19 November).
[29] S. Kilpimaa, H. Runtti, U. Lassi, T.T. Kuokkanen, Chemical activation of gasification carbon residue for phosphate removal, porous media and its applications in science, engineering and industry, AIP Conference Proceedings (2012) 293–298.
[30] A. Bhatnagar, A.K. Minocha, M. Sillanpää, Adsorptive removal of cobalt from aqueous solution by utilizing lemon peel as biosorbent, Biochem. Eng. J. 48 (2010) 181–186.
[31] D. Özçimen, A. Ersoy-Meriçboyu, Removal of copper from aqueous solutions by adsorption onto chestnut shell and grapeseed activated carbons, J. Hazard. Mater. 168 (2009) 1118–1125.
[32] J.P. Chen, X. Wang, Removing copper, zinc, and lead ion by granular activated carbon in pretreated fixed-bed columns, Sep. Purif. Technol. 19 (2000) 157–167.
[33] E.-Z. El-Ashtoukhy, N.K. Amin, O. Abdelwahab, Removal of lead (II) and copper (II) from aqueous solution using pomegranate peel as a new adsorbent, Desalination 223 (2008) 162–173.
[34] C.A. Rozaini, K. Jain, C.W. Oo, K.W. Tan, L.S. Tan, A. Azraa, K.S. Tong, Optimization of nickel and copper ions removal by modified mangrove barks, Int. J. Chem. Eng. Appl. 1 (2010) 84–89.
[35] I. Langmuir, The adsorption of gases on plane surfaces of glass, mica and platinum, J. Am. Chem. Soc. 40 (1918) 1361–1403.
[36] H.M.F. Freundlich, Over the adsorption in solution, J. Phys. Chem. 57 (1906) 385–470.
[37] V. Vadivelan, K.V. Kumar, Equilibrium, kinetics, mechanism, and process design for the sorption of methylene blue onto rice husk, J. Colloid Interface Sci. 286 (2005) 90–100.
[38] E.M. McCasc, Surface Chemistry, New York, Oxford, 2007.
[39] J. Memon, S.Q. Memon, M.I. Bhanger, M.Y. Khuhawar, Use of modified sorbent for the separation and preconcentration of chromium species from industrial waste water, J. Hazard. Mater. 163 (2009) 511–516.
[40] J.L. Sotelo, G. Ovejero, A. Rodríguez, S. Álvarez, J. García, Analysis and modeling of fixed bed column operations on flumequine removal onto activated carbon: pH influence and desorption studies, Chem. Eng. J. 228 (2013) 102–113.
[41] S. Lagergren, About the theory of so-called adsorption of soluble substances, K. Svenska. Vetenskapsakad. Handl. 24 (1898) 1–39.
[42] Y.S. Ho, G. McKay, Pseudo-second order model for sorption processes, Process Biochem. 34 (1999) 451–465.

[43] W.J. Weber Jr., J.C. Morris, Kinetics of adsorption on carbon from solution, J. Sanit. Eng. Div. 89 (1963) 31–59.
[44] M.A. Hossain, H.H. Ngo, W.S. Guo, T. Setiadi, Adsorption and desorption of copper(II) ions onto garden grass, Bioresour. Technol. 121 (2012) 386–395.
[45] M. Kapur, M.K. Mondal, Competitive sorption of Cu(II) and Ni(II) ions from aqueous solutions: kinetics, thermodynamics and desorption studies, J. Taiwan Inst. Chem. E (2014) 1803–1813.
[46] J.L. Zhou, P.L. Huang, R.G. Lin, Sorption and desorption of Cu and Cd by macroalgae and microalgae, Environ. Pollut. 101 (1998) 67–75.
[47] W.D. Schecher, D.C. McAvoy, MINEQL+: A Chemical Equilibrium Modeling System, Version 4.5 for Windows, User's Manual, second ed., Hallowell, Maine, 2003.
[48] C.F. Baes Jr., R.E. Mesmer, Hydrolysis of Cations, John Wiley, New York (N.Y.), 1976.
[49] C. Faur-Brasquet, Z. Reddad, K. Kadirvelu, P. Le Cloirec, Modeling the adsorption of metal ions (Cu^{2+}, Ni^{2+}, Pb^{2+}) onto ACCs using surface complexation models, Appl. Surf. Sci. 196 (2002) 356–365.
[50] K. Anoop Krishnan, K.G. Sreejalekshmi, R.S. Baiju, Nickel(II) adsorption onto biomass based activated carbon obtained from sugarcane bagasse pith, Bioresour. Technol. 102 (2011) 10239–10247.
[51] A. Ewecharoen, P. Thiravetyan, E. Wendel, H. Bertagnolli, Nickel adsorption by sodium polyacrylate-grafted activated carbon, J. Hazard. Mater. 171 (2009) 335–339.
[52] H. Hasar, Adsorption of nickel(II) from aqueous solution onto activated carbon prepared from almond husk, J. Hazard. Mater. 97 (2003) 49–57.
[53] S. Kilpimaa, T. Kuokkanen, U. Lassi, Characterization and utilization potential of wood ash from combustion process and carbon residue from gasification process, BioRes 8 (1) (2013) 1011–1027.
[54] M. Uğurlu, I. Kula, M.H. Karaoğlu, Y. Arslan, Removal of Ni(II) ions from aqueous solutions using activated-carbon prepared from olive stone by $ZnCl_2$ activation, Environ. Prog. Sustain. Energy 28 (2009) 547–557.
[55] I. Kula, M. Uğurlu, M.H. Karaoğlu, A. Çelik, Adsorption of Cd(II) ions from aqueous solution using activated carbon prepared from olive stone by $ZnCl_2$ activation, Bioresour. Technol. 99 (2008) 492–501.
[56] J.C. Moreno, R. Gómez, L. Giraldo, Removal of Mn, Fe, Ni and Cu ions from wastewater using cow bone charcoal, Materials 3 (2010) 452–466.
[57] U. Kouakou, A.S. Ello, J.A. Yapo, A. Trokourey, Adsorption of iron and zinc on commercial activated carbon, J. Environ. Chem. Ecotoxicol. 5 (2013) 168–171.
[58] A. Sheibani, M.R. Shishehbor, H. Alaei, Removal of Fe(III) ions from aqueous solution by hazelnut hull as an adsorbent, Int. J. Ind. Chem. 3 (2012) 1–4.
[59] A.H. Hawari, C.N. Mulligan, Biosorption of lead(II), cadmium(II), copper(II) and nickel(II) by anaerobic granular biomass, Bioresour. Technol. 97 (2006) 692–700.
[60] A. Papandreou, C.J. Stournaras, D. Panias, Copper and cadmium adsorption on pellets made from fired coal fly ash, J. Hazard. Mater. 148 (2007) 538–547.
[61] E. López, B. Soto, M. Arias, A. Núñez, D. Rubinos, M.T. Barral, Adsorbent properties of red mud and its use for wastewater treatment, Water Res. 32 (1998) 1314–1322.
[62] M.H. Kalavathy, T. Karthikeyan, S. Rajgopal, L.R. Miranda, Kinetic and isotherm studies of Cu(II) adsorption onto H_3PO_4-activated rubber wood sawdust, J. Colloid Interface Sci. 292 (2005) 354–362.
[63] V.K. Gupta, I. Ali, Utilisation of bagasse fly ash (a sugar industry waste) for the removal of copper and zinc from wastewater, Sep. Purif. Technol. 18 (2000) 131–140.
[64] M.H. Kalavathy, B. Karthik, L.R. Miranda, Removal and recovery of Ni and Zn from aqueous solution using activated carbon from *Hevea brasiliensis*: batch and column studies, Colloids Surf. B: Biointerfaces 78 (2010) 291–302.
[65] H. Parab, S. Joshi, N. Shenoy, A. Lali, U.S. Sarma, M. Sudersanan, Determination of kinetic and equilibrium parameters of the batch adsorption of Co(II), Cr(III) and Ni(II) onto coir pith, Process Biochem. 41 (2006) 609–615.
[66] S. Basha, Z.V.P. Murthy, B. Jha, Sorption of Hg(II) onto *Carica papaya*: experimental studies and design of batch sorber, Chem. Eng. J. 147 (2009) 226–234.
[67] G. McKay, H.S. Blair, J.R. Gardner, Adsorption of dyes on chitin. I. Equilibrium studies, J Appl. Polym. Sci. 27 (1982) 3043–3057.
[68] M. Ghasemi, M. Naushad, N. Ghasemi, Y. Khosravi-fard, Adsorption of Pb(II) from aqueous solution using new adsorbents prepared from agricultural waste: adsorption isotherm and kinetic studies, J. Ind. Eng. Chem. 20 (2014) 2193–2199.
[69] A. Bhatnagar, E. Kumar, M. Sillanpää, Nitrate removal from water by nano-alumina: characterization and sorption studies, Chem. Eng. J. 163 (2010) 317–323.
[70] M. Pirilä, M. Martikainen, K. Ainassaari, T. Kuokkanen, R.L. Keiski, Removal of aqueous As(III) and As(V) by hydrous titanium dioxide, J. Colloid Interface Sci. 353 (2011) 257–262.
[71] F. Wu, R. Tseng, R. Juang, Comparisons of porous and adsorption properties of carbons activated by steam and KOH, J. Colloid Interface Sci. 283 (2005) 49–56.
[72] J.M. Dias, M.C.M. Alvim-Ferraz, M.F. Almeida, J. Rivera-Utrilla, M. Sánchez-Polo, Waste materials for activated carbon preparation and its use in aqueous-phase treatment: a review, J. Environ. Manage. 85 (2007) 833–846.